Different primary thyroid B-cell lymphomas show overlapping mutation profiles, suggesting involvement of a common pathogenic process

Maria-Myrsini Tzioni,[1] Natsuko Watanabe,[2] Ellen Stelloo,[3] Zi Chen,[1] Adheesh Ghosh,[4] Fangtian Wu,[1] Kiminori Sugino,[5] Koichi Ito,[5] Harma Feitsma,[3] Manabu Fujisawa,[6,7] Mamiko Sakata-Yanagimoto,[6,8,9] Lívia Rásó-Barnett,[10] Teresa Marafioti,[4,11] Ayoma D Attygalle,[12] Andrew Wotherspoon[12] and Ming-Qing Du[1]

[1]Department of Pathology, University of Cambridge, Cambridge, UK; [2]Department of Internal Medicine, Ito Hospital, Tokyo, Japan; [3]Cergentis BV, Utrecht, the Netherlands; [4]Cancer Institute, University College London, London, UK; [5]Department of Surgery, Ito Hospital, Tokyo, Japan; [6]Department of Hematology, Institute of Medicine, University of Tsukuba, Ibaraki, Japan; [7]Centre for Lymphoid Cancer, BC Cancer, Vancouver, British Columbia, Canada; [8]Department of Hematology, University of Tsukuba Hospital, Ibaraki, Japan; [9]Division of Advanced Hemato-Oncology, Transborder Medical Research Center, University of Tsukuba, Ibaraki, Japan; [10]The Haematopathology and Oncology Diagnostic Service, Addenbrookes Hospital, Cambridge, UK; [11]Department of Cellular Pathology, University College London Hospitals NHS Foundation Trust, London, UK and [12]Department of Histopathology, The Royal Marsden Hospital, London, UK

Correspondence: Ming-Qing Du
mqd20@cam.ac.uk

Received: May 28, 2025.
Accepted: March 6, 2026.
Early view: March 19, 2026.

https://doi.org/10.3324/haematol.2025.288239

Published under a CC BY license

Abstract

Primary thyroid lymphomas commonly originate from a background of Hashimoto's thyroiditis and comprise largely extranodal marginal zone lymphoma of mucosa-associated lymphoid tissue (EMZL), diffuse large B-cell lymphoma (DLBCL), and follicular lymphoma (FL). Thyroid EMZL harbors a distinct mutation profile, but whether this discriminates them from thyroid FL and DLBCL is unknown. To investigate this, we have examined 42 EMZL (11 *BCL6*-translocation [tr]+ve), 21 FL (5 *BCL2*-tr+ve, 10 *BCL6*-tr+ve, 1 both *BCL2/BCL6*-tr+ve) and 34 DLBCL of the thyroid. Targeted next generation sequencing revealed a remarkable overlap in the mutation profile among thyroid EMZL, *BCL2*-tr-ve FL and DLBCL, all showing frequent mutations in *TET2, IGLL5, TNFRSF14, CD274, GNA13, FAS, KLF2* and *TNFAIP3*. In contrast, *BCL2*-tr+ve FL of the thyroid showed frequent *BCL2, KMT2D, CREBBP, EZH2*, but not *TET2* and *CD274* mutations. Genomic analysis of *BCL6* translocation by targeted locus capture next generation sequencing showed different genomic configurations between thyroid FL and EMZL. In thyroid FL, the majority of *BCL6* translocations placed its coding exons under the transcriptional control of the *IGH* switch region super-enhancer or its partner genes, potentially resulting in *BCL6* constitutive expression. In contrast, the majority of *BCL6* translocations in thyroid EMZL juxtaposed the *BCL6* gene to the IGHJ/D region without encompassing the Eμ enhancer or its partner genes in an opposite orientation, thus less likely to lead to constitutive BCL6 transactivation. The above genetic changes likely dysregulate B-cell maturation and peripheral tolerance, thus offer significant molecular insights into the pathogenesis of thyroid lymphomas, particularly underpinning autoimmunity in the lymphomagenesis and potentially explaining the overlap in histopathology between EMZL and FL.

Introduction

Primary thyroid lymphomas commonly originate from a background of chronic lymphocytic thyroiditis (Hashimoto's thyroiditis, HT) and comprise largely extranodal marginal zone lymphoma of mucosa-associated lymphoid tissue (EMZL), diffuse large B-cell lymphoma (DLBCL), and followed by follicular lymphoma (FL).[1] The histological diagnosis of these thyroid lymphomas can be readily made by integrated histological and immunophenotypic assessment in most cases. However, a high proportion of thyroid FL are negative for *BCL2* translocation and lack expression of CD10. These cases often pose significant problems in differential diagnosis from thyroid EMZL that frequently show prominent follicular colonization, hence considerable overlap in their morphological and immunophenotypic presentations.[2]

We previously showed that thyroid EMZL had a distinct mutation profile characterized by concurrent mutations in *TET2*, *CD274* (PD-L1) and *TNFRSF14*, distinguishing them from those of other B-cell lymphomas including EMZL at other anatomic sites.[3-5] However, the genetic profile of thyroid FL and DLBCL remains to be unravelled, particularly whether there is any difference in the genetic profile between thyroid FL and EMZL, and if so, whether such genetic differences can help their differential diagnosis. In addition, *BCL6* translocation is occasionally seen in EMZL, but seemingly more frequent in those of the thyroid.[6-8] This is rather paradoxical given that BCL6 functions as a master regulator of the germinal center (GC) reaction, preventing GC B-cell exit by repressing the plasma cell differentiation program.[9,10] To address these questions, and to further understand the pathogenesis of thyroid lymphomas, we performed targeted next generation sequencing (NGS) of 172 lymphoma genes and integrated analyses in a large cohort of primary thyroid lymphoma including 42 EMZL, 21 FL and 34 DLBCL. We also investigated the genomic configuration of *BCL6* translocation in thyroid FL and EMZL by targeted locus capture NGS in order to understand the paradoxical finding of *BCL6* translocation in thyroid EMZL.

Methods

Patients and clinical data

A total of 97 cases of primary thyroid B-cell lymphoma (94 from Ito Hospital, Tokyo) were successfully investigated, including 24 cases of EMZL that had been previously studied.[3] The histological diagnosis was reviewed with the help of additional immunohistochemistry (*Online Supplementary Table S1*) and interphase fluorescence *in situ* hybridization for *BCL2* and *BCL6* translocations by expert hematopathologists (AW and ADA). The final diagnosis compromised 42 EMZL (11 with *BCL6* translocation), 21 FL (5 with *BCL2* translocation, 10 with *BCL6* translocation, 1 case with both *BCL2* and *BCL6* translocations, 5 lacking both *BCL2* and *BCL6* translocations) and 34 DLBCL (*Online Supplementary Table S2*).

The use of archival tissues for research was approved by the ethics committees of the institutions involved in the study.

DNA extraction and quality assessment

In each case, tumor rich areas (>30%) were microdissected on formalin-fixed paraffin-embedded (FFPE) tissue slides. DNA was extracted and assessed for quality by polymerase chain reaction (PCR) of variably sized genomic fragments as previously described.[11]

Mutation analysis by targeted next generation sequencing

The target panel included 172 genes recurrently mutated in MZL, FL and DLBCL (*Online Supplementary Table S3*). FFPE tissue DNA (100ng) were fragmented using the Covaris E220 Focused Ultrasonicator (Covaris, Brighton, UK). For each DNA sample, an indexed library was prepared using the xGen™ UDI-UMI indexes (IDT, Coralville, IA, USA) and pooled for target enrichment using TWIST probes (TWIST Biosciences, San Francisco, CA, USA). The enriched DNA targets were amplified by PCR and then pooled together for sequencing using the Illumina NextSeq 2000 platform (2x100bp paired-end sequencing protocol). The sequence data analysis, variant calling, and filtering were performed as described in our previous studies.[12,13]

For DNA sample with suboptimal quality (PCR amplification of genomic fragment ≤300bp), targeted sequencing was performed in duplicate and only variants detected by both replicates were considered as a true change (*Online Supplementary Figure S1*).

Mutation signature analysis

This analysis was based on all somatic single base substitutions including synonymous, non-synonymous, splice site and UTR changes using Sigprofiler assignment.[14]

Genomic analysis of chromosome translocation by next generation sequencing

The genomic configuration of *BCL6* translocation was investigated by targeted locus capture next generation sequencing (TLC-NGS) as described previously and a customized NGS panel (*Online Supplementary Methods and Online Supplementary Table S4*).[15] The *IGH* genomic segments including super enhancer positions were according to those described previously using the hg19 assembly.[16]

Re-analysis of single-cell RNA-sequencing data from mice germinal center B cells

TET2 inactivation by mutation may cause genome-wide hypermethylation, hence potentially impact on gene expression in B cells and their phenotype. To explore this, we revisited the single cell sequencing data from a previous mouse study.[17]

Germinal center B cells sorted from the spleens of tumor-bearing Tet2-deficient (MxTR) and wild-type (MxWT) mice were used for library preparation for RNA sequencing (RNA-seq: MxRT, N=5; MxWT, N=4) and whole-genome bisulfite sequencing (WGBS: MxTR, N=2; MxWT, N=2). Sequencing data were reanalyzed as previously described.[17] Differential expression data from RNA-seq were analyzed using DESeq2.[18] The methylation rate of each base by WGBS was visualized in the UCSC Genome Browser.

Statistical analysis

The comparison of mutation load and gene expression among different groups was assessed using Wilcoxon Rank-Sum test with two-sided *P* values. Association between mutation frequencies and clinical parameters among

lymphoma groups and their subsets was examined using the Fisher exact test. Mutation association was analyzed using the somaticInteractions function in the Maftools R Bioconductor package.[19]

Results

Histopathological and immunophenotypic features of thyroid lymphoma

In comparison with EMZL of other sites, thyroid cases showed prominent follicular colonizations, albeit to a variable extent in some cases. Among the 40 cases of thyroid EMZL with complete CD21, CD10 and BCL6 immunohistochemistry data, 38 showed extensive follicular colonization, predominantly type 1 (poorly defined follicle/mantle zone) or type 2 (follicle and mantle zone variably preserved) pattern in 24 and 14 cases, respectively.[20] Irrespective of different follicular colonization patterns, 30 cases showed virtually absent CD10 expression in all or most colonized follicles, albeit variable BCL6 staining (Figure 1). The remaining 8 cases showed a mixed pattern with some of the colonized follicles displaying partial CD10 positivity consistent with the presence of residual GC B cells.

With the exception of one case (grade 3B), all other thyroid FL were grade 3A (Figure 2C), and all showed predominantly a nodular growth pattern, and also prominent lymphoepithelial lesions including “MALT balls” (Figure 2). Like classic

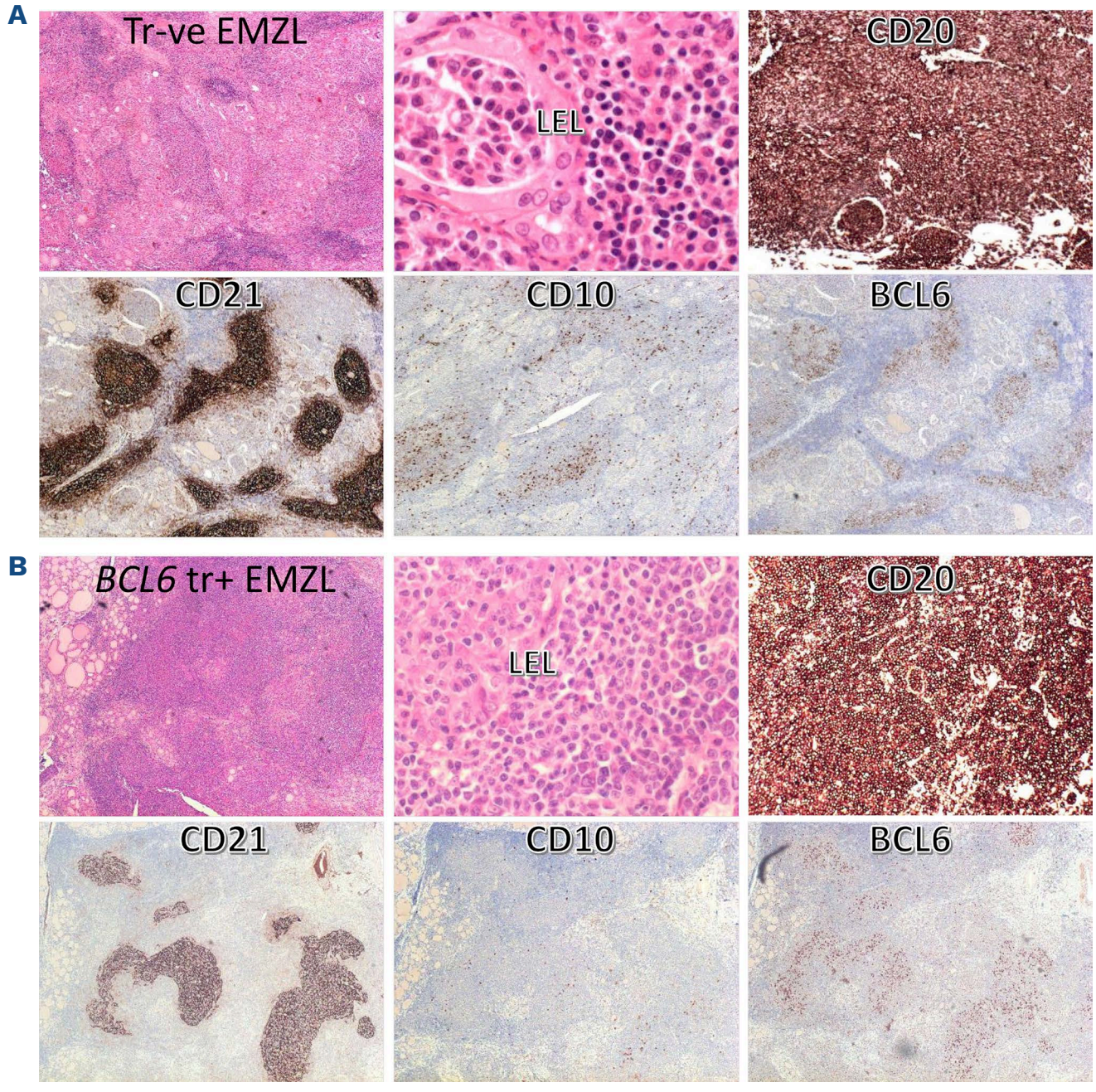


Figure 1. Histopathology of a representative primary thyroid extranodal marginal zone lymphoma of mucosa-associated lymphoid tissue. (A) A thyroid extranodal marginal zone lymphoma of mucosa-associated lymphoid tissue (EMZL) without *BCL6* translocation (case EMZL-37) shows diffuse infiltration of neoplastic B cells with prominent lymphoepithelial lesions including “MALT ball”, and also extensive follicular colonization. CD10 immunohistochemistry highlights residual germinal center (GC) B cells, while neoplastic B cells in the colonized follicle are CD10 negative. BCL6 positivity likely identifies both residual GC B cells and the colonized neoplastic B cells. (B) A thyroid EMZL with *BCL6* translocation (case EMZL-04) displays diffuse infiltration of neoplastic B cells with prominent lymphoepithelial lesions. CD21 immunohistochemistry highlights the colonized follicles that are virtually negative for CD10 but show variable BCL6 expression, indicating total overrun by neoplastic B cells. tr+ve: translocation positive, tr-ve: translocation negative; LEL: lymphoepithelial lesion. Magnification 40x for the 2 images that show LEL; magnification 4x for all other low power images.

FL, *BCL2*-translocation [tr]+ve thyroid FL expressed both CD10 and BCL6, albeit a single case with both *BCL2* and *BCL6* translocations was CD10 negative (Figure 2). Of the 15 *BCL2*-tr-ve FL, only 6 showed CD10 expression, with the

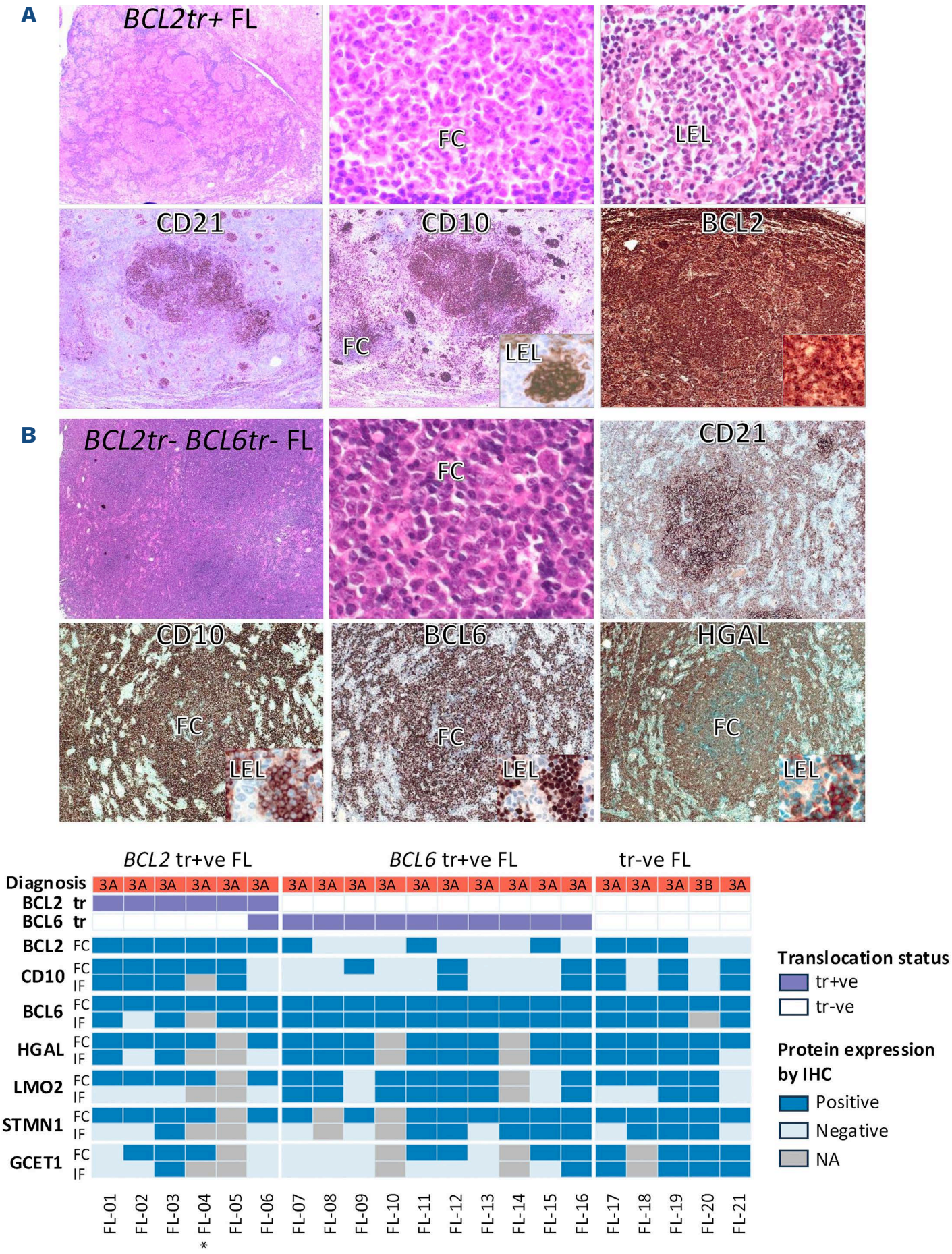


Figure 2. Histopathology of representative primary thyroid follicular lymphoma. (A) A *BCL2* translocation positive follicular lymphoma (FL) (case FL-05) shows follicular growth pattern and extensive lymphoepithelial lesions (LEL) including "MALT ball" in the interfollicular region (IF). The neoplastic cells including those involved in the LEL are strongly positive for CD10 and BCL2. Magnification: top, left = 2x; top, middle and right = 40x. Bottom = 4x (insert, LEL = 40x). (B) A *BCL2* and *BCL6* translocation negative FL (case FL-19) displays vaguely follicular growth pattern with little involvement of the IF. The neoplastic B cells in both the follicle center (FC) and IF are positive for CD10, BCL6 and HGAL. Magnification: top, left = 2x; top, middle = 40x; all other panels = 4x (insert, LEL = 40x). (C) Summary of immunophenotype of primary thyroid FL. CD10 is more often negative in *BCL2* translocation negative FL including those with *BCL6* translocation. *FL-04 showed no apparent neoplastic involvement in the IF. IHC: immunohistochemistry; NA: not available; STMN1: Stathmin 1; tr+ve: translocation positive; tr-ve: translocation negative.

remaining cases negative for CD10 including 7 and 2 with and without *BCL6* translocation, respectively (Figure 2B, C). The FL diagnosis in these cases, including those negative for both *BCL2* and *BCL6* translocations, was supported by observation of expression of other GC markers (BCL6, HGAL, LMO2, GCET1, STMN1) in neoplastic B cells within and outside B-cell follicles (Figure 2B, *Online Supplementary Figure S2*). In contrast, none of these GC markers was positive in the neoplastic B cells outside B-cell follicles in 21 cases of thyroid EMZL examined.

Thyroid DLBCL were unremarkable; all were negative for *BCL2* translocation and 4 had *BCL6* translocation. Of the 34 cases investigated, 27 and 17 showed BCL6 and CD10 expression by immunohistochemistry, respectively.

Mutation signature among different thyroid B-cell lymphomas

All somatic variants including synonymous, non-synonymous, indels and UTR changes were included in the mutation load analysis (*Online Supplementary Table S5*). Overall, the mutation load was significantly higher in DLBCL than FL (P=0.006) and EMZL (P=0.005), but there was no significant difference between the two latter groups (Figure 3A). As many of the genes (N=37) investigated are targets of the somatic hypermutation (SHM) process, a separate analysis of mutations in these genes was performed, and this showed a similar trend, with DLBCL cases having a significantly higher mutation load in SHM targets than FL (P=0.021) and EMZL (P=0.014) (Online Supplementary Figure S3).

We next compared the mutation signature among the three lymphoma groups by combining all the somatic single base substitutions of each group together as none of the individual cases had a sufficient number of variants for such analysis. As expected, the cytidine deaminase (AID) associated mutation signature SBS84 was similarly found among the three lymphoma groups (*Online Supplementary Figure S3*).[21] Similarly, the clock-like/age-related mutation signature SBS5 was also high among the three lymphoma groups.[21]

Mutation profile among different thyroid B-cell lymphomas

The pathogenic mutations were compared among the three lymphoma groups with subset analysis according to translocation status.

Remarkably, there was a considerable overlap in the overall mutation profile among thyroid EMZL, *BCL2*-tr-ve FL and DLBCL, with frequent mutations in *TET2, IGLL5, TNFRSF14, CD274, GNA13, KLF2, TNFAIP3* and *FAS* (Figures 3A and 4A, *Online Supplementary Figures S4 and S5*). Such an overlap in mutation profile among the three groups was also seen in the genes not targeted by the SHM process (Figure 4A, *Online Supplementary Figure S4*). Apart from a few genes, there was no significant difference in the mutation frequencies of the vast majority of genes between EMZL and *BCL2*-tr-ve FL, nor between *BCL2*-tr-ve FL and DLBCL (Figures 3B and 4A). Similarly, there was no significant difference in the mutation profile between *BCL2*-tr-ve FL with and without *BCL6* translocation, nor between EMZL with and without *BCL6* translocation (Figure 3B, *Online Supplementary Figure S6*). Nonetheless, thyroid DLBCL showed a significantly higher incidence of mutation than thyroid EMZL in several genes (*SGK1, KLHL6, B2M, EBF1, SOCS1, FOXO1, P2RY8, DUSP2, KRAS, CD58*) (Figures 3B and 4A).

In contrast, *BCL2*-tr+ve FL of the thyroid showed frequent *BCL2, KMT2D, CREBBP, EZH2, TNFRSF14*, but not *TET2, CD274* and *IGLL5* mutations (Figures 3B and 4A), similar to the mutation profile of nodal FL.[22] Nonetheless, all these thyroid cases were associated with HT as evidenced by clinical, laboratory and histological investigations, with 4/5 cases at early stage (IE=2, IIE=2), supporting their thyroid origin (*Online Supplementary Table S2*).

Analysis of co-occurrence of the mutations revealed a number of significant associations and mutual exclusions (Figure 4B). For example, *TET2* mutation was significantly associated with changes in *CD274, TNFAIP3, TNFRSF14* and *IGLL5*, and *CD274* mutation was further significantly associated with changes in *TNFRSF14, PABPC1, TNFAIP3, FAS* and *KLF2*, but mutually exclusive from changes in *KLHL6* and *B2M* (Figure 4B).

Distinct genomic configuration of *BCL6* translocation between thyroid follicular lymphoma and extranodal marginal zone lymphoma of mucosa-associated lymphoid tissue

The genomic configuration of *BCL6* translocation in 8 FL and 10 EMZL were investigated by TLC-NGS, and a further 2 FL were studied by a customized NGS panel (Figures 5 and 6).

Among the 10 FL with *BCL6* translocation, 3 showed genomic fusion between the *BCL6* intron 1 and the centromeric *IGHA1* region including 3'regulatory region 1 (3'RR1) super-enhancer in the same orientation, and this genomic configuration may cause *BCL6* transactivation due to super-enhancer hijack[23] (Figure 5). A further 5 cases displayed genomic fusion between *BCL6* intron 1 or its upstream 5'UTR region and either the 5' regions of partner genes (*HSP90AA1, HMGA1, ZBTB38*) or the 3'UTR of *MIR29A* in the same orientation, and these genomic configurations represented a promoter substitution thus placing *BCL6* under the transcriptional control of its translocation partner. In the remaining 2 cases, one showed fusion between the BCL6 intron 1 and the centromeric *IGHJ6* region in the same orientation, and the juxtaposed *IGHJ* region did not contain the Eμ super enhancer, thus lacking the apparent mechanism to transactivate *BCL6* expression. In the other case, the translocation placed an upstream region of the *BCL6* gene between the *IGH* and *IGK*, and the translocation did not involve any *BCL6* coding exons, thus unlikely

affecting BCL6 expression (Figure 5).

Among the 10 *BCL6*-tr+ve EMZL, 5 cases showed genomic fusion between *BCL6* intron-1 or its upstream 5'UTR region, and the centromeric region of *IGHJ6* or D2-8 in the

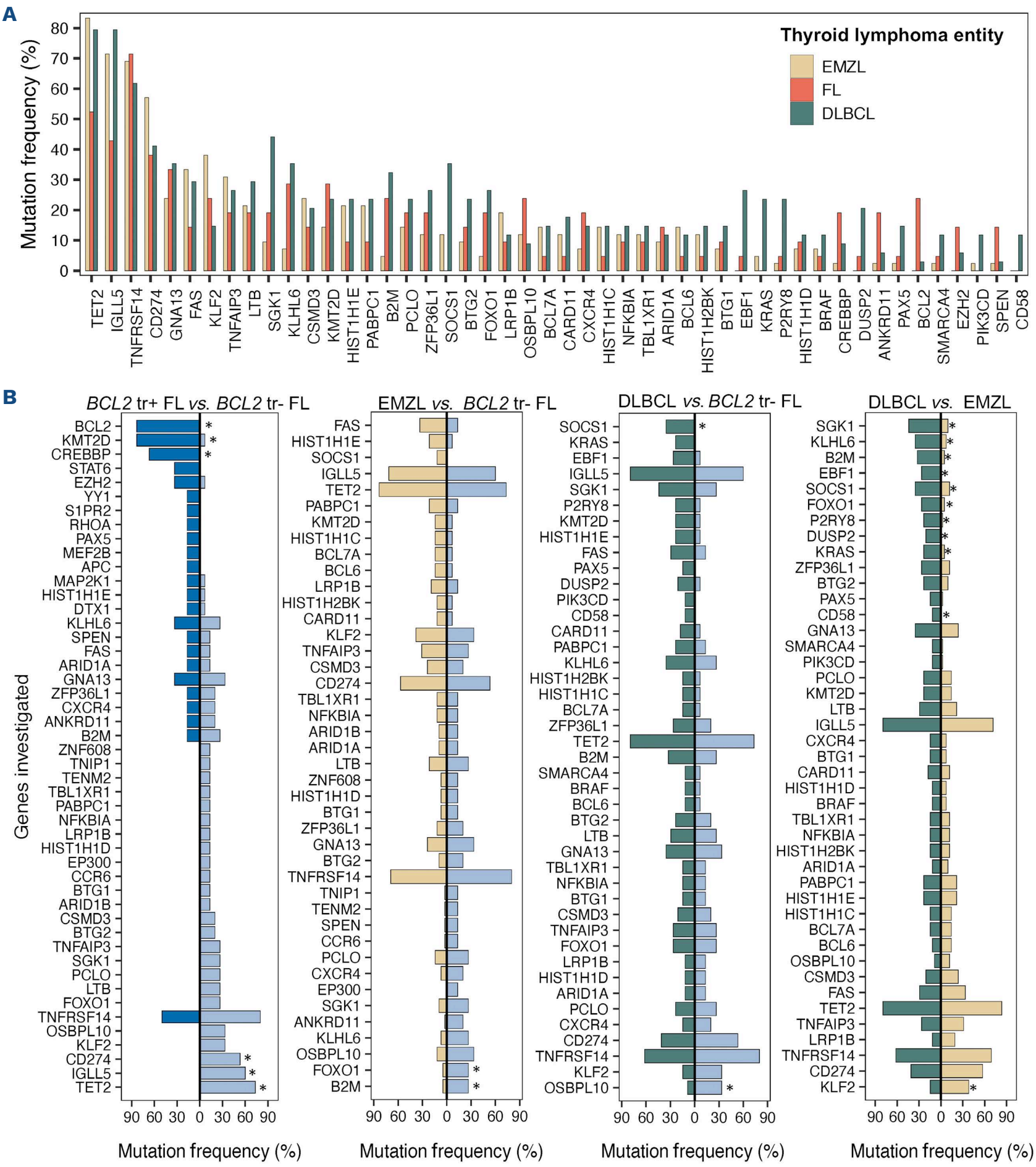


Figure 3. Comparison of mutation frequencies among different primary thyroid lymphomas. (A) Comparison of mutation frequencies among thyroid extranodal marginal zone lymphoma of mucosa-associated lymphoid tissue (EMZL), follicular lymphoma (FL) and diffuse large B-cell lymphoma (DLBCL). Only genes showing a frequency of potentially pathogenic mutation above 10% in any of these lymphoma groups are included, with the exception of *BCL2*, of which all variants are included. (B) Comparison of mutation frequency between subsets of thyroid EMZL, FL and DLBCL as indicated. In each comparison, all genes showing a mutation frequency above 10% in any of the two subsets included, with the exception of *BCL2*, of which all variants are included to highlight different mutation profiles among various comparisons. *Significant changes between subsets ($P \leq 0.05$). tr+ve: translocation positive; tr-ve: translocation negative.

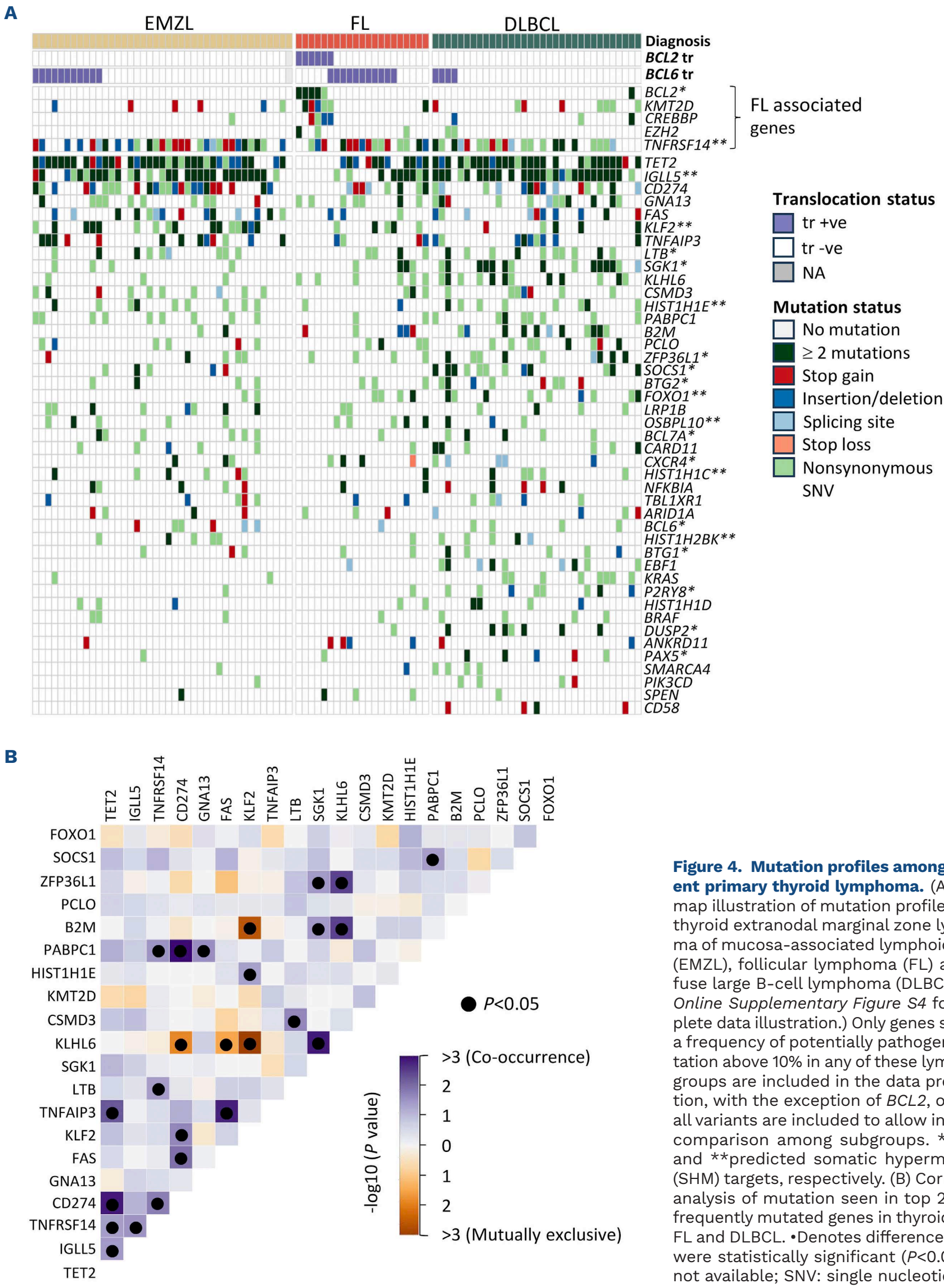


Figure 4. Mutation profiles among different primary thyroid lymphoma. (A) Heatmap illustration of mutation profile among thyroid extranodal marginal zone lymphoma of mucosa-associated lymphoid tissue (EMZL), follicular lymphoma (FL) and diffuse large B-cell lymphoma (DLBCL). (See *Online Supplementary Figure S4* for complete data illustration.) Only genes showing a frequency of potentially pathogenic mutation above 10% in any of these lymphoma groups are included in the data presentation, with the exception of *BCL2*, of which all variants are included to allow informed comparison among subgroups. *Known and **predicted somatic hypermutation (SHM) targets, respectively. (B) Correlation analysis of mutation seen in top 20 most frequently mutated genes in thyroid EMZL, FL and DLBCL. •Denotes differences which were statistically significant ($P<0.05$). NA: not available; SNV: single nucleotide variation; tr+ve: translocation positive; tr-ve: translocation negative.

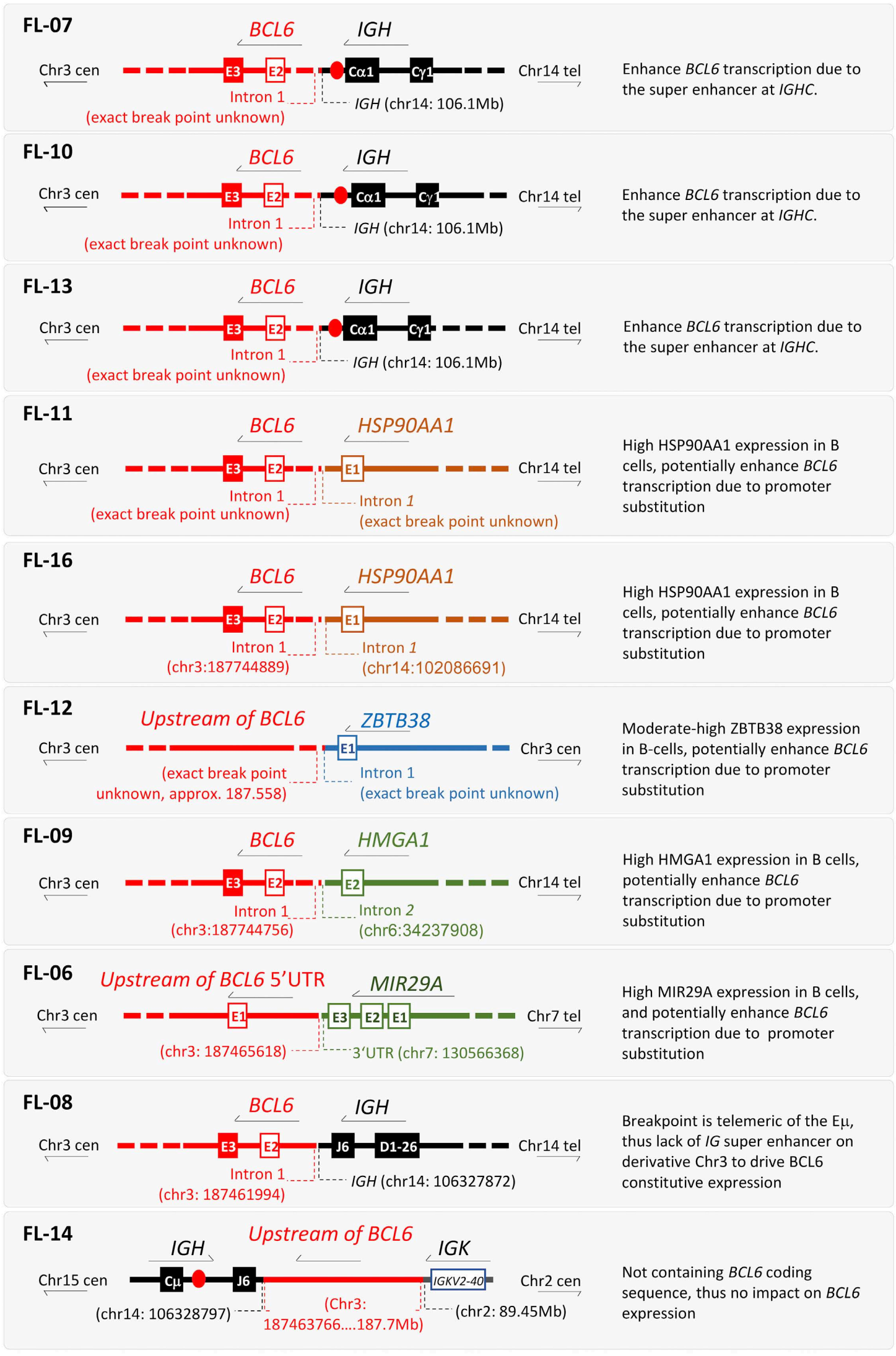


Figure 5. Genomic configuration of *BCL6* translocation in primary thyroid follicular lymphoma. Genomic breakpoint sequencing analysis was performed by targeted locus capture-based next generation sequencing (TLC-NGS) or a customized NGS panel with sequence annotations based on human genome (hg19) together with IGH super enhancers according to Mikulasova *et al.*[16] cen: centromeric; tel: telomeric.

same orientation (Figure 6). As the translocated *IGHJ* and D2-8 region did not contain the Eμ super enhancer, these translocations lacked any apparent mechanism to drive constitutive *BCL6* expression. A further 2 cases displayed genomic fusion between the upstream of the *BCL6* 5'UTR region and its partner gene (upstream of *GRHPR* or upstream of *IGLL5*) in an opposite orientation, with no obvious evidence of super-enhancer hijack that may drive constitutive *BCL6* transactivation (Figure 6). In the remaining 3 cases, the translocation fused the *BCL6* 5'UTR or intron 1 to different partner genes in the same orientation (intron 2 of *SGK1* and *GAPDH* and intron 1 of *SMC4*), with the latter one potentially representing a promoter substitution.

In addition, TLC-NGS also identified additional chromosome translocations in 4 cases of the above *BCL6*-tr+ve thyroid lymphomas, including 3 FL and one EMZL (*Online Supplementary Figure S7*). One of these FL showed *IGH*::*BCL2* and the other 2 revealed an *IGH* involved translocation, one in association with *BTG2* but not involving its coding exons, and the remaining one in association with *IGK*. The EMZL case showed *IGH*::*SOX5*, with genomic configuration potentially driving *SOX5* expression (*Online Supplementary Figure S7*).

Potential impact of genetic changes on follicular lymphoma phenotype

As many of the genes frequently altered in primary thyroid lymphoma are critical for the GC B-cell development, these genetic changes may potentially affect the maturation process of GC B cells, hence determining their differentiation stages that undergo malignant transformation. To investigate this, we first examined the expression pattern of *TET2, CD274, TNFRSF14, BCL6* and *MME* (CD10) in various normal GC B-cell subsets using the single cell transcriptomic data from human tonsils.[24] Interestingly, these genes showed a similar trend of expression across different GC B-cell subsets, being abundantly expressed in proliferating dark zone (DZ) GC B cells, reaching the highest expression level in DZ non-proliferating GC B cells and DZ to LZ (light zone) transition cells, then decreasing to the lowest level in LZ proliferating and LZ-to-DZ transition GC B-cell subsets (Figure 7).

The expression of the above genes must be tightly regulated, and their coordinated alterations are deemed critical in GC B-cell maturation and peripheral tolerance. As *TET2* mutation in primary thyroid lymphoma is an early event,[3,5] its inactivation by mutations may cause genome-wide hypermethylation, thus potentially affect the above gene expression. To explore this, we examined this gene expression in *Tet2* deficient mouse GC B cells from a previous study.[17] In comparison with the wild-type mouse GC B cells, the *Tet2* deficient mouse GC B cells showed a higher level of methylation in *Irf4* (promoter), *Cd274* (gene body, introns) and *Mme* (CD10) (CpG site), and a reduced expression of these genes (Figure 8). However, there was no significant alteration in the methylation profile and expression of *Tnfrsf14* in the *Tet2* deficient mouse GC B cells.

Correlation analysis of clinical, pathological and genetic data

A history of HT was present at a similar rate among thyroid EMZL (38/40; 95%), FL (17/21; 81%) and DLBCL (28/34; 82%) (*Online Supplementary Table S2*). The average duration of HT was significantly higher in *BCL6*-tr-ve EMZL than the *BCL6*-tr+ve EMZL (P=0.008). Apart from that the DLBCL group showed a significant higher level of serum LDH than EMZL (P=0.005), and elevated sIL-2R than both FL (P=0.005) and EMZL (P=0.0000022), there were no significant differences among the standard clinical and laboratory parameters including TgAb and TPOAb among the three lymphoma groups.

Discussion

By investigating the genetic changes of primary thyroid EMZL, FL and DLBCL, we have unravelled several novel observations. 1) Apart from *BCL2*-tr+ve FL, there is a remarkable overlap in the mutation profile among *BCL2*-tr-ve FL, EMZL, and DLBCL of the thyroid. 2) The core of these commonly mutated genes involves *TET2, TNFRSF14* and *CD274*, distinguishing them from other B-cell lymphomas, including those at other mucosal sites. 3) *BCL6* translocation is recurrently seen in both thyroid FL and EMZL, but there is a fundamental difference in its genomic configuration between the two lymphoma entities. As many of these frequent genetic changes target genes that regulate B-cell maturation and tolerance in the peripheral lymphoid tissues, the above novel findings offer significant molecular insights into the pathogenesis of these thyroid lymphomas.

Like nodal FL, thyroid *BCL2*-tr+ve FL showed frequent mutations in *BCL2, TNFRSF14, KMT2D, CREBBP* and *EZH2*. Intriguingly, none of these thyroid *BCL2*-tr+ve FL showed *TET2* and *CD274* mutations. It is important to note that these *BCL2*-tr+ve FL were associated with HT, and mainly at early clinical stages, not secondary to a systemic nodal disease. As *BCL2* translocation is an early event in FL development, occurring at the pre-B cell stage due to erroneous *IGH* VDJ recombination, it is pertinent to speculate that the aberrant BCL2 overexpression caused by the translocation may favor the subsequent genetic changes with cooperative oncogenic activities, thus giving rise to a unique mutation pattern seen in all *IGH*::*BCL2* positive neoplasms, including *in situ* follicular B-cell neoplasm, FL and transformed FL.[12,25-29]

The remarkable overlap in the mutation profile (*TET2, IGLL5, TNFRSF14, CD274, GNA13, KLF2, TNFAIP3, FAS*) (Figure 3A) among *BCL2*-tr-ve FL, EMZL and DLBCL of the thyroid is intriguing, but biologically plausible. As these lymphomas originate from a common background of HT, their develop-

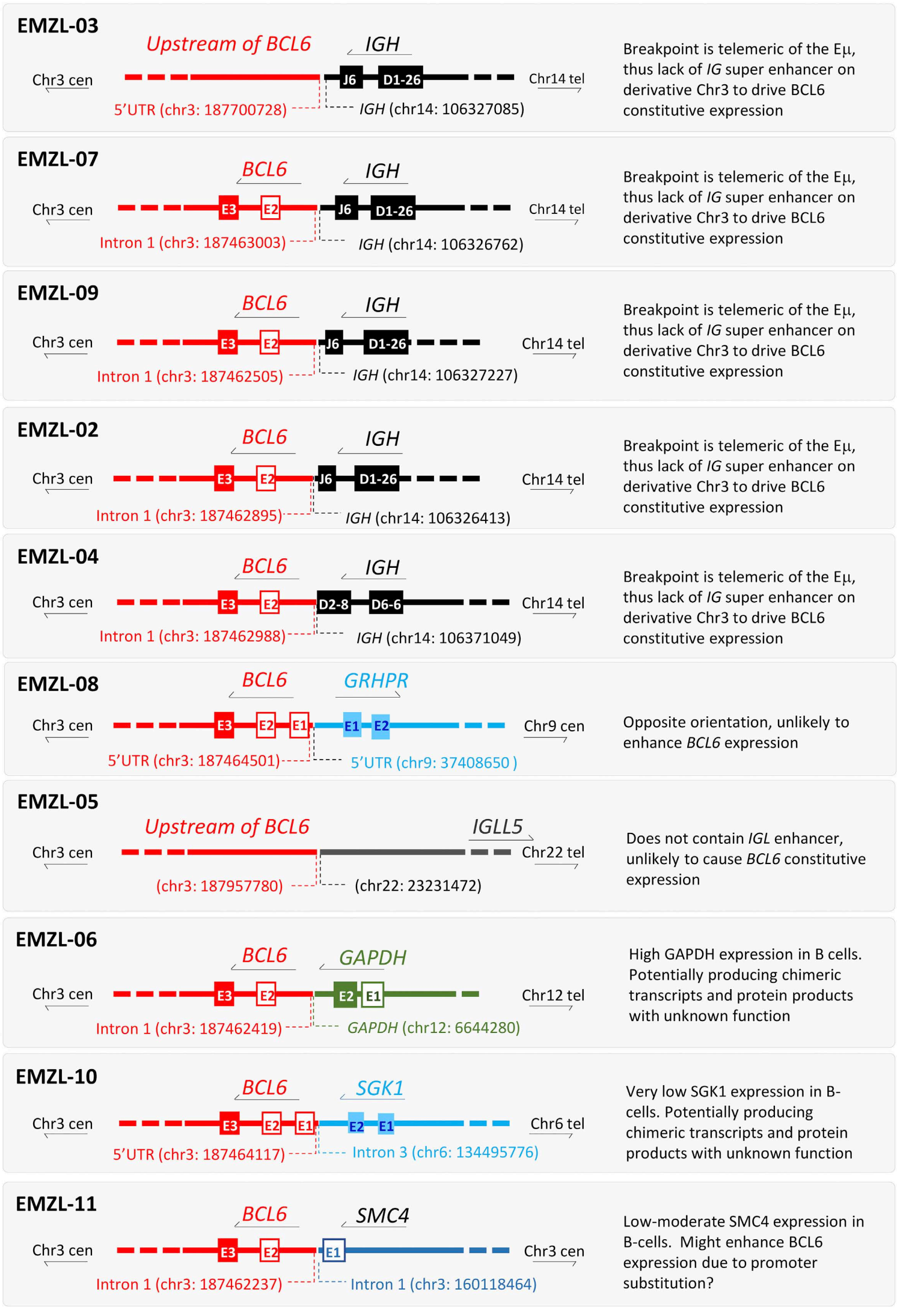


Figure 6. Genomic configuration of BCL6 translocation in primary thyroid extranodal marginal zone lymphoma of mucosa-associated lymphoid tissue. Genomic breakpoint sequencing analyses was performed by targeted locus capture-based next generation sequencing (TLC-NGS) with sequence annotations based on human genome (hg19) together with IGH super enhancers according to Mikulasova et al.16 cen: centromeric; tel: telomeric.

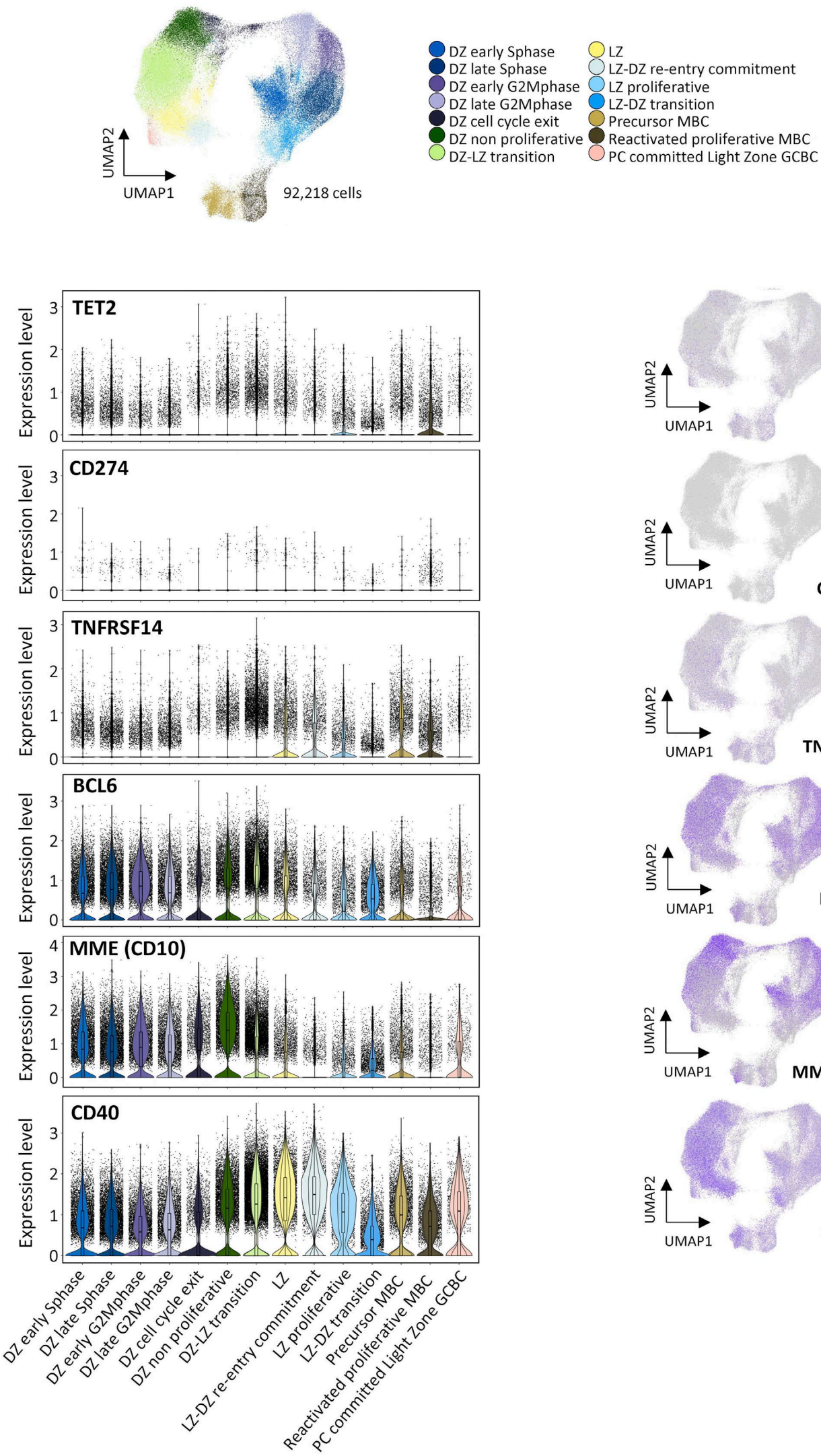


Figure 7. Re-analyses of single-cell RNA sequencing data of germinal centre (GC) B cells from the tonsil cell atlas project.[24] UMAP illustration shows the overall distribution of the indicated genes among various subsets of germinal center B cells (GC B cells). Violin plots with overlaid box plots compare the expression level of the indicated genes (TET2, CD274, TNFRSF14, BCL6, MME [CD10], and CD40) among various subsets of GC B cells. DZ: dark zone; LZ: light zone; MBC: memory B cells; PC: plasma cells.

ment most likely involves the same pathological process of autoimmunity that underpins HT. HT is characterized by development of autoreactive B cells, and histologically extensive GC reactions, a process critically depending on T-helper cells. The molecular mechanisms that underpin the breach of peripheral tolerance may drive the evolution of autoreactive B cells and their clonal expansion. As B cells undergo reiterative GC reactions and relentless exposure to SHM activities, this may lead to acquisition of genetic abnormalities and eventual malignant transformation. In this context, the occurrence of malignant B-cell clone can be viewed as a part of the overall autoimmune process, but as an extreme presentation. Thus, the overlapping mutation profile among *BCL2*-tr-ve FL, EMZL and DLBCL of the thyroid is likely driven by their common etiology, i.e., the pivotal pathological process associated with HT.

In support of the above speculation, several genes among those frequently mutated in thyroid lymphoma are involved in the governance of peripheral tolerance. *CD274* (PD-L1) and *TNFRSF14* encode ligands for co-inhibitory surface receptor PD1 and BTLA on T-helper cells, respectively, and their inactivation by somatic mutation/deletion most likely constrain their negative regulation on T-helper cell function. PD-L1 deficiency or impairing PD1/PD-L1 interaction can cause autoimmune disorders in animal models.[30,31] Similarly, immune checkpoint inhibitors, particularly anti-PD1 antibody, frequently cause cancer patients to develop autoimmune thyroiditis and/or autoantibodies including anti-thyroperoxidase and anti-thyroglobulin.[32,33] Moreover, patients with germline *PD1* or *CD274* (PD-L1) loss-of-function mutations show early-onset endocrine autoimmunity.[34,35] *Cd274* deficiency in B cells appears to promote T-helper cell function, consequently enabling B cells a growth advantage.[36,37] Similarly, *Tnfrsf14* deficient B cells gain an enhanced growth advantage due to exaggerated T-cell help through increased CD40/CD40L co-stimulation.[38,39] The concurrent inactivation of both *CD274* (PD-L1) and *TNFRSF14* in thyroid lymphomas may synergise in their enhancement of T-helper cell function, thus breaching peripheral tolerance and providing growth advantage to autoreactive B cells.

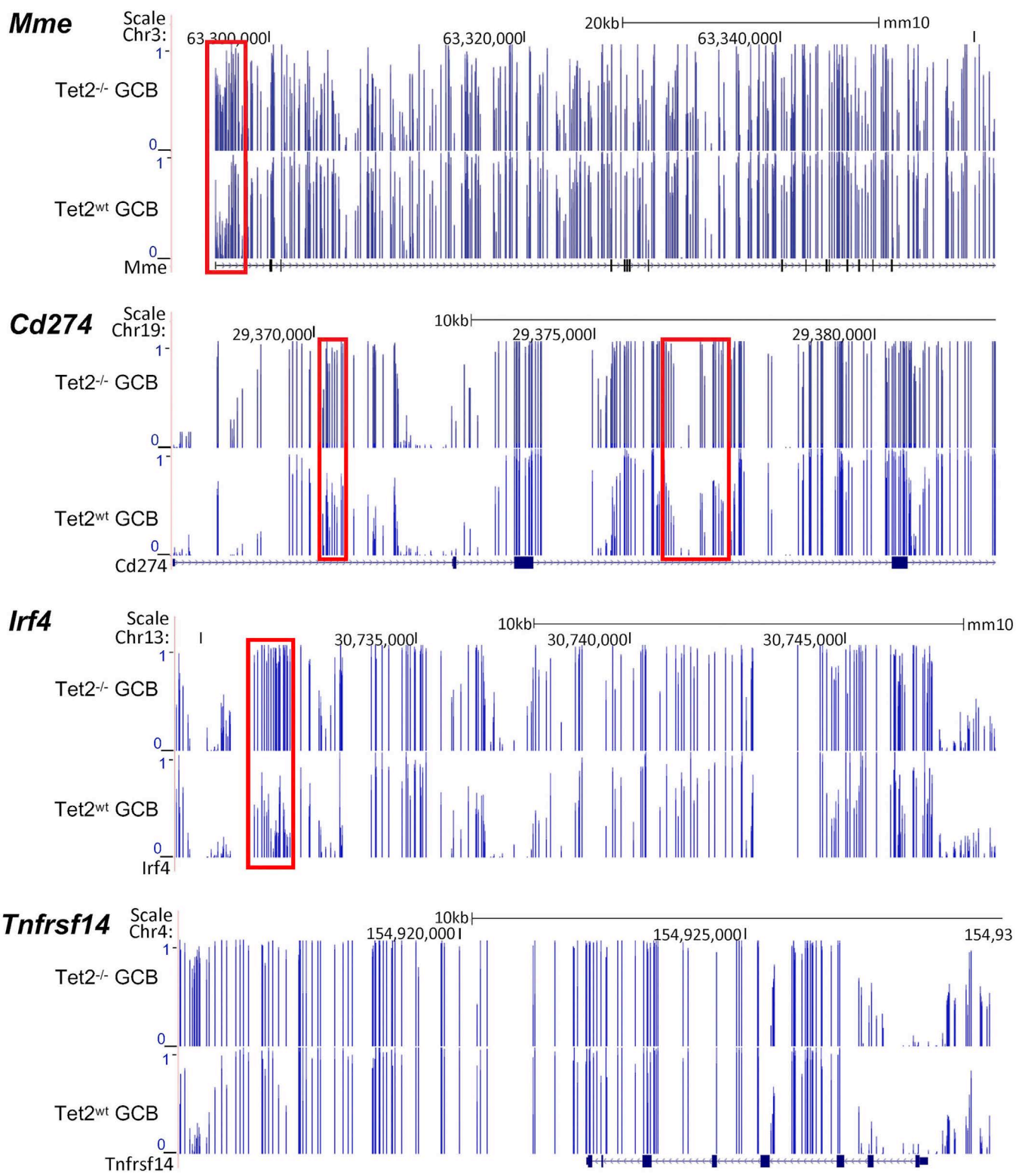
The above lymphomagenic process is likely augmented by the concurrent loss-of-function mutations in *TNFAIP3, KLF2* and *FAS. TNFAIP3* encodes a global negative regulator of the canonical NF-βB activation pathway and attenuates signaling transduction from several surface receptors, including BCR, TNFR, TLR and IL1βR, by inactivating their downstream signaling molecules through its ubiquitin editing activities.[40] Similarly, *KLF2* encodes a transcription factor/repressor that can negatively regulate NF-βB and NOTCH2 activities triggered by a range of surface receptor signaling.[41] *FAS* encodes a surface receptor for apoptosis signaling and mutant *FAS* can act as a dominant-negative, preventing FAS interaction with its downstream adaptor molecule FADD to mediate apoptosis.[42] Taken together, TNFAIP3, KLF2 and FAS inactivation may promote the apoptosis evasion of autoreactive B cells and their clonal expansion.[43]

The above mutations may also have a major impact on the histological presentation of lymphoma. Deficiency of *Tnfrsf14* or *Cd274* alone increases GC B-cell competitiveness in mice.[36,38] A combined inactivation of both *CD274* (PD-L1) and *TNFRSF14* in B cells may significantly enhance their entry, expansion and retention in B-cell follicles due to enhanced T-helper cell signals.[31] These biological impacts may underpin the follicular growth pattern of thyroid FL as well as the extensive follicular colonization of thyroid EMZL. In this context, it is pertinent to point out that follicular colonization in thyroid EMZL is the most prominent among EMZL of various sites, often involving most or the majority of B-cell follicles, thus posing significant difficulty in differential diagnosis from *BCL2*-tr-ve FL.[2]

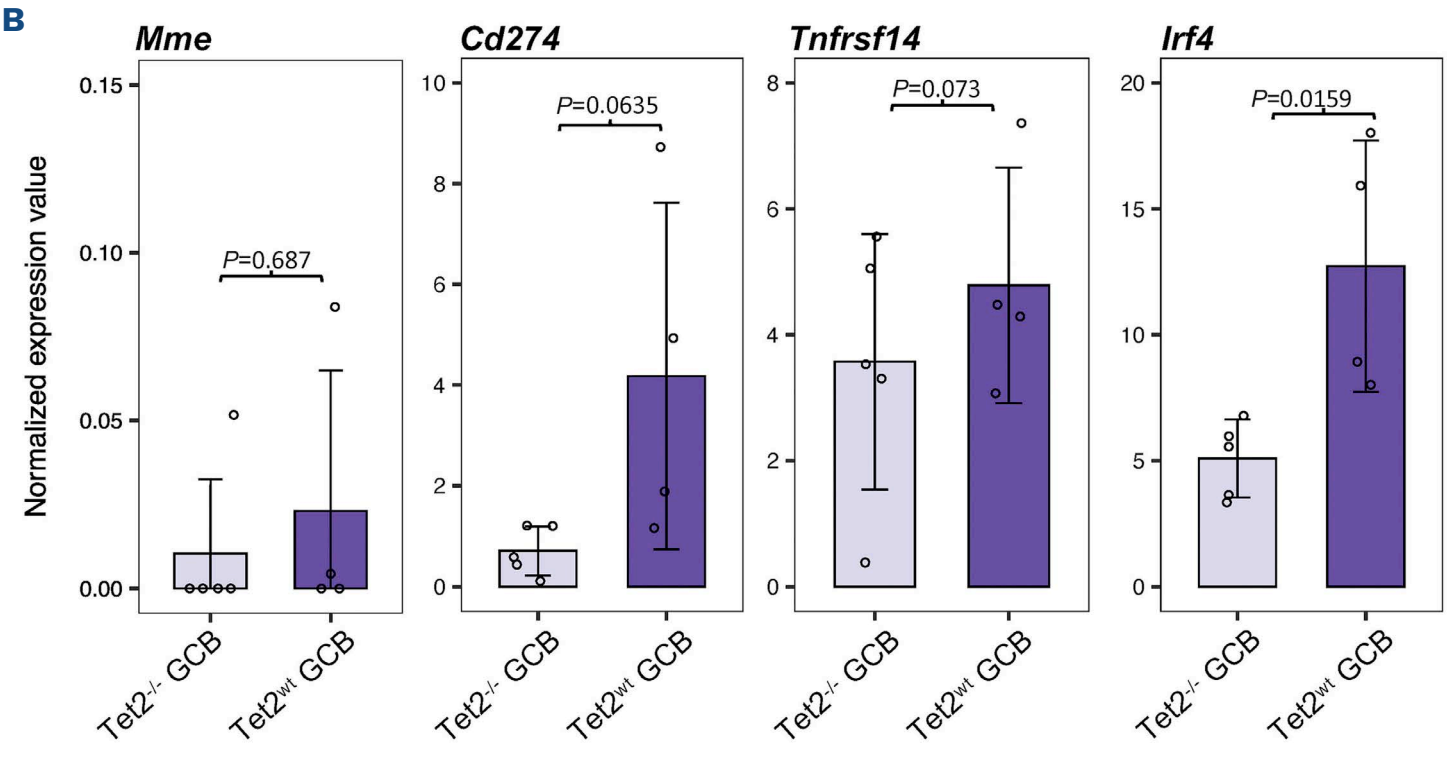
In a similar context, pediatric-type follicular lymphoma (PTFL) and pediatric nodal marginal zone lymphoma (PNMZL) also exhibit substantial overlap in their clinical, morphological and genetic features.[44,45] The shared genetic changes between the two lymphomas have been used to argue for considering these different lymphomas to be a single biological entity with variations in their histological presentations.[44,45] The somatic genetic alterations and tumor microenvironmental factors that influence GC entry (for example T-cell dependent B-cell activation) and GC exit (via BCL6 downregulation) are likely to have a major impact on the phenotypic presentation of these lymphomas. However, studies so far have largely focused on mutations within coding gene sequences, while other potentially relevant genetic changes, such as somatic mutations in *BCL6* transcriptional regulatory (non-coding) regions that could affect GC exit,[46,47] have still to be explored. Thus, the currently available data are not sufficient to support considering these lymphomas as a single biological entity.

The finding of recurrent *BCL6* translocation in EMZL is rather paradoxical as BCL6 is a master transcriptional factor that orchestrates the GC reaction while repressing the plasma cell differentiation program,[9,10] hence maintaining the GC phenotype. Our finding of significant differences in the genomic configuration of *BCL6* translocation between thyroid FL and EMZL provides a plausible explanation. In thyroid FL, the majority of *BCL6* translocations place the *BCL6* coding exons under the transcriptional control of the *IGH* switch region super enhancer (3'RR1) or its partner genes, known as super enhancer hijack and promoter substitution, respectively. Among the 5 cases with *BCL6* translocation genomic configuration showing promoter substitution, all the partner genes (*HSP90AA1, HMGA1, ZBTB38, MIR29A*) appear to be highly expressed in B cells.[48-53] These genomic configurations most likely enable *BCL6* constitutive expression. In contrast, the majority of

A



B



Continued on following page.

Figure 8. Epigenomic and transcriptomic alterations in germinal center B cells from Tet2-deficient and wild-type mice. (A) Visualizations of base-resolution DNA methylation profiles at representative gene loci (*Mme, Cd274, Irf4*, and *Tnfrsf14*) derived from whole-genome bisulfite sequencing (WGBS) of germinal center (GC) B cells sorted from the spleens of *Tet2*-deficient ($Tet2^{-/-}$) and wild-type ($Tet2^{wt}$) mice. The y-axis represents base-resolution methylation levels derived from WGBS. Differentially methylated regions (q-value ≤ 0.25 and |methylation difference| > 30%) are highlighted with red squares. (B) Normalized expression values of the indicated genes based on DESeq2 analysis of RNA-sequencing data ($Tet2^{-/-}$, N=5; $Tet2^{wt}$, N=4).[17,18]

BCL6 translocations in thyroid EMZL juxtapose the *BCL6* gene to the *IGHJ/IGHD* region without encompassing the Eμ enhancer or partner genes in an opposite orientation. In the 3 cases of thyroid EMZL where *BCL6* is placed in the same orientation with its partner gene, 2 cases involved coding exons of the partner gene (*GAPDH, SGK1*), potentially resulting in chimeric transcripts and possible protein products with unknown function; the remaining case with the partner gene *SMC4* may represent a true promoter substitution, but SMC4 appears not to be highly expressed in B cells.[49,50] Overall, BCL6 translocation in thyroid EMZL lacks the apparent genomic configuration that enables *BCL6* constitutive expression, hence minimal impact on the lymphoma phenotypic presentation.

TET2, CD274 and *TNFRSF14* inactivation may also affect the GC B-cell maturation process, potentially influencing their differentiation stage that undergoes malignant transformation, and hence the neoplastic cell immunophenotype. As shown in tonsils, during normal GC reaction, the downregulation of *CD274* and *TNFRSF14* expression in LZ centrocytes may dampen their inhibitory effect on T-follicular helper cells, allowing them to receive more T-cell help, preparing for GC exit or re-entry to DZ for further SHM. *Tet2* deficiency increased the proportion of GC centrocytes and impaired GC exit.[54] Although the molecular mechanism of how *Tet2* deficiency dysregulates the GC reaction is not fully understood, *Tet2* deficient mouse GC B cells showed an increased level of DNA methylation in *Cd274, Mme* (CD10) and *Irf4*, accompanied by their reduced expression in comparison with wild-type controls.[17] This, together with the inactivation of both *CD274* and *TNFRSF14*, may promote the GC B-cell maturation process toward LZ centrocytes and memory B-cell differentiation. On the other hand, *BCL6* constitutive expression by translocation and/or other mechanisms may prevent the late GC B cells from GC exit by repressing transcription factors (BLIMP1) that are critical for plasma cell differentiation.[9,10] Taken together, it is conceivable that these genetic changes may cooperate in their oncogenic activities, promoting the GC B-cell differentiation process but impairing their GC exit, thus favoring malignant transformation of the late GC B-cell subsets. This may potentially explain why a high proportion of *BCL2*-tr-ve FL of the thyroid is CD10 negative.

In conclusion, our findings offer significant molecular insights into the pathogenesis of thyroid lymphomas, bridging autoimmunity, somatic genetic changes and lymphomagenesis together, and potentially explain the overlap of histological presentations between thyroid EMZL and FL.

Disclosures

ES and HF are employees of Cergentis BV, the company that developed the Targeted Locus Capture (TLC) technology used in this study. All the other authors have no conflicts of interest to disclose.

Contributions

M-MT is responsible for FISH, targeted NGS, immunohistochemistry data collection and analyses, and prepared and wrote the manuscript; M-QD is responsible for FISH, targeted NGS, immunohistochemistry data collection and analyses, case contribution and pathology, study conception, coordination and research funding, and prepared and wrote the manuscript; NW is responsible for study conception, coordination and research funding, case contribution and pathology; ES, HF, ZC, AG, FW and TM are responsible for FISH, targeted NGS, immunohistochemistry data collection and analyses; MF and MS-Y are responsible for mouse experimental data; KS, KI, LR-B, ADA and AW are responsible for case contribution and pathology. All authors contributed to manuscript preparation and writing, and read and approved the final version of the manuscript for publication.

Acknowledgments

The authors would like to thank Dr. Ana Toribio and Jessica Ferreira Gouveia for their assistance with Illumina sequencing.

Funding

The study was supported by research grants from Blood Cancer UK (22011, 24011, 19011, 19010), Cancer Research UK (CRCBPA-Nov23/100001, C8333/A29707) and an International Collaborative Award from the Pathological Society of Great Britain and Ireland, UK (ICA 1019 01). M-MT was supported by a BBSRC DTP PhD studentship (BBSRC BB/M011194/1). MF was supported by Gilead's Research Scholars Program and The Leukemia & Lymphoma Society (3442-25). The Human Research Tissue Bank of the Cambridge University Hospitals NHS Foundation Trust is supported by the NIHR Cambridge Biomedical Research Centre.

Data-sharing statement

All core data generated or analyzed during this study are included in this published article, and additional raw data are available from the corresponding author on reasonable request.

References

1. Watanabe N, Noh JY, Narimatsu H, et al. Clinicopathological features of 171 cases of primary thyroid lymphoma: a long-term study involving 24 553 patients with Hashimoto's disease. Br J Haematol. 2011;153(2):236-243.
2. Bacon CM, Diss TC, Ye H, et al. Follicular lymphoma of the thyroid gland. Am J Surg Pathol. 2009;33(1):22-34.
3. Wu F, Watanabe N, Tzioni MM, et al. Thyroid MALT lymphoma: self-harm to gain potential T-cell help. Leukemia. 2021;35(12):3497-3508.
4. Moody S, Thompson JS, Chuang SS, et al. Novel GPR34 and CCR6 mutation and distinct genetic profiles in MALT lymphomas of different sites. Haematologica. 2018;103(8):1329-1336.
5. Tzioni MM, Watanabe N, Chen Z, et al. Primary thyroid B-cell lymphoma: molecular insights into its clonal evolution and relapse. J Pathol. 2025;265(2):123-131.
6. Ye H, Remstein ED, Bacon CM, Nicholson AG, Dogan A, Du MQ. Chromosomal translocations involving BCL6 in MALT lymphoma. Haematologica. 2008;93(1):145-146.
7. Dierlamm J, Pittaluga S, Stul M, et al. BCL6 gene rearrangements also occur in marginal zone B-cell lymphoma. Br J Haematol. 1997;98(3):719-725.
8. Suzuki A, Hirokawa M, Higashiyama T, et al. Flow cytometric, gene rearrangement, and karyotypic analyses of 110 cases of primary thyroid lymphoma: a single-institutional experience in Japan. Endocr J. 2019;66(12):1083-1091.
9. Parekh S, Polo JM, Shaknovich R, et al. BCL6 programs lymphoma cells for survival and differentiation through distinct biochemical mechanisms. Blood. 2007;110(6):2067-2074.
10. Shapiro-Shelef M, Lin KI, Mcheyzer-Williams LJ, Liao J, Mcheyzer-Williams MG, Calame K. Blimp-1 is required for the formation of immunoglobulin secreting plasma cells and pre-plasma memory B cells. Immunity. 2003;19(4):607-620.
11. Cucco F, Clipson A, Kennedy H, et al. Mutation screening using formalin-fixed paraffin-embedded tissues: a stratified approach according to DNA quality. Lab Invest. 2018;98(8):1084-1092.
12. Cucco F, Barrans S, Sha C, et al. Distinct genetic changes reveal evolutionary history and heterogeneous molecular grade of DLBCL with MYC/BCL2 double-hit. Leukemia. 2019;34(5):1329-1341.
13. Zhang C, Stelloo E, Barrans S, et al. Non-IG::MYC in diffuse large B-cell lymphoma confers variable genomic configurations and MYC transactivation potential. Leukemia. 2024;38(3):621-629.
14. Díaz-Gay M, Vangara R, Barnes M, et al. Assigning mutational signatures to individual samples and individual somatic mutations with SigProfilerAssignment. Bioinformatics. 2023;39(12):btad756.
15. Allahyar A, Pieterse M, Swennenhuis J, et al. Robust detection of translocations in lymphoma FFPE samples using targeted locus capture-based sequencing. Nat Commun. 2021;12(1):3361.
16. Mikulasova A, Kent D, Trevisan-Herraz M, et al. Epigenomic translocation of H3K4me3 broad domains over oncogenes following hijacking of super-enhancers. Genome Res. 2022;32(7):1343-1354.
17. Fujisawa M, Nguyen TB, Abe Y, et al. Clonal germinal center B cells function as a niche for T-cell lymphoma. Blood. 2022;140(18):1937-1950.
18. Love MI, Huber W, Anders S. Moderated estimation of fold change and dispersion for RNA-seq data with DESeq2. Genome Biol. 2014;15(12):550.
19. Mayakonda A, Lin DC, Assenov Y, Plass C, Koeffler HP. Maftools: efficient and comprehensive analysis of somatic variants in cancer. Genome Res. 2018;28(11):1747-1756.
20. Isaacson PG, Androulakis-Papachristou A, Diss TC, Pan L, Wright DH. Follicular colonization in thyroid lymphoma. Am J Pathol. 1992;141(1):43-52.
21. Alexandrov LB, Kim J, Haradhvala NJ, et al. The repertoire of mutational signatures in human cancer. Nature. 2020;578(7793):94-101.
22. Perrett M, Edmondson C, Okosun J. Biology of follicular lymphoma: insights and windows of clinical opportunity. Hematology Am Soc Hematol Educ Program. 2022;2022(1):688-694.
23. Kasprzyk ME, Sura W, Dzikiewicz-Krawczyk A. Enhancing B-cell malignancies-on repurposing enhancer activity towards cancer. Cancers (Basel). 2021;13(13):3270.
24. Massoni-Badosa R, Aguilar-Fernández S, Nieto JC, et al. An atlas of cells in the human tonsil. Immunity. 2024;57(2):379-399.e18.
25. Okosun J, Bödör C, Wang J, et al. Integrated genomic analysis identifies recurrent mutations and evolution patterns driving the initiation and progression of follicular lymphoma. Nat Genet. 2014;46(2):176-181.
26. Pasqualucci L, Khiabanian H, Fangazio M, et al. Genetics of follicular lymphoma transformation. Cell Rep. 2014;6(1):130-140.
27. Bouska A, Zhang W, Gong Q, et al. Combined copy number and mutation analysis identifies oncogenic pathways associated with transformation of follicular lymphoma. Leukemia. 2017;31(1):83-91.
28. Kridel R, Chan FC, Mottok A, et al. Histological transformation and progression in follicular lymphoma: a clonal evolution study. PLoS Med. 2016;13(12):e1002197.
29. Dobson R, Wotherspoon A, Liu SA, et al. Widespread in situ follicular neoplasia in patients who subsequently developed follicular lymphoma. J Pathol. 2022;256(4):369-377.
30. Sage PT, Schildberg FA, Sobel RA, Kuchroo VK, Freeman GJ, Sharpe AH. Dendritic cell PD-L1 limits autoimmunity and follicular T cell differentiation and function. J Immunol. 2018;200(8):2592-2602.
31. Martinov T, Swanson LA, Breed ER, et al. Programmed death-1 restrains the germinal center in type 1 diabetes. J Immunol. 2019;203(4):844-852.
32. Chalan P, Di Dalmazi G, Pani F, De Remigis A, Corsello A, Caturegli P. Thyroid dysfunctions secondary to cancer immunotherapy. J Endocrinol Invest. 2018;41(6):625-638.
33. De Moel EC, Rozeman EA, Kapiteijn EH, et al. Autoantibody development under treatment with immune-checkpoint inhibitors. Cancer Immunol Res. 2019;7(1):6-11.
34. Ogishi M, Kitaoka K, Good-Jacobson KL, et al. Impaired development of memory B cells and antibody responses in humans and mice deficient in PD-1 signaling. Immunity. 2024;57(1):2790-2807.e15.
35. Johnson MB, Ogishi M, Domingo-Vila C, et al. Human inherited PD-L1 deficiency is clinically and immunologically less severe than PD-1 deficiency. J Exp Med. 2024;221(6):e20231704.
36. Shi J, Hou S, Fang Q, Liu X, Liu X, Qi H. PD-1 controls follicular T helper cell positioning and function. Immunity. 2018;49(2):264-274.e4.
37. Wan Z, Lin Y, Zhao Y, Qi H. TFH cells in bystander and cognate interactions with B cells. Immunol Rev. 2019;288(1):28-36.
38. Mintz MA, Felce JH, Chou MY, et al. The HVEM-BTLA axis

restrains T cell help to germinal center B cells and functions as a cell-extrinsic suppressor in lymphomagenesis. Immunity. 2019;51(2):310-323.e7.
39. Kennedy R, Klein U. A T cell-B cell tumor-suppressive axis in the germinal center. Immunity. 2019;51(2):204-206.
40. Du MQ. MALT lymphoma: a paradigm of NF-κB dysregulation. Semin Cancer Biol. 2016;39:49-60.
41. Clipson A, Wang M, De Leval L, et al. KLF2 mutation is the most frequent somatic change in splenic marginal zone lymphoma and identifies a subset with distinct genotype. Leukemia. 2015;29(5):1177-1185.
42. Consonni F, Gambineri E, Favre C. ALPS, FAS, and beyond: from inborn errors of immunity to acquired immunodeficiencies. Ann Hematol. 2022;101(3):469-484.
43. Du MQ. EMZL at various sites: learning from each other. Blood. 2025;145(19):2117-2127.
44. Salmeron-Villalobos J, Egan C, Borgmann V, et al. A unifying hypothesis for PNMZL and PTFL: morphological variants with a common molecular profile. Blood Adv. 2022;6(16):4661-4674.
45. Lim S, Lim KY, Koh J, et al. Pediatric-type indolent B-cell lymphomas with overlapping clinical, pathologic, and genetic features. Am J Surg Pathol. 2022;46(10):1397-1406.
46. Saito M, Gao J, Basso K, et al. A signaling pathway mediating downregulation of BCL6 in germinal center B cells is blocked by BCL6 gene alterations in B cell lymphoma. Cancer Cell. 2007;12(3):280-292.
47. Bal E, Kumar R, Hadigol M, et al. Super-enhancer hypermutation alters oncogene expression in B cell lymphoma. Nature. 2022;607(7920):808-815.
48. Liston A, Papadopoulou AS, Danso-Abeam D, Dooley J. MicroRNA-29 in the adaptive immune system: setting the threshold. Cell Mol Life Sci. 2012;69(21):3533-3541.
49. Schmiedel BJ, Singh D, Madrigal A, et al. Impact of genetic polymorphisms on human immune cell gene expression. Cell. 2018;175(6):1701-1715.e16.
50. Monaco G, Lee B, Xu W, et al. RNA-seq signatures normalized by mRNA abundance allow absolute deconvolution of human immune cell types. Cell Rep. 2019;26(6):1627-1640.e7.
51. Wong R, Bhattacharya D. ZBTB38 is dispensable for antibody responses. PLoS One. 2020;15(9):e0235183.
52. Tan LP, Wang M, Robertus JL, et al. miRNA profiling of B-cell subsets: specific miRNA profile for germinal center B cells with variation between centroblasts and centrocytes. Lab Invest. 2009;89(6):708-716.
53. De Martino M, Esposito F, Fusco A. Critical role of the high mobility group A proteins in hematological malignancies. Hematol Oncol. 2022;40(1):2-10.
54. Dominguez PM, Ghamlouch H, Rosikiewicz W, et al. TET2 deficiency causes germinal center hyperplasia, impairs plasma cell differentiation, and promotes B-cell lymphomagenesis. Cancer Discov. 2018;8(12):1632-1653.